

Third-order nonlinear optical response and photoluminescence characterization of tellurite glasses with different alkali metal oxides as network modifiers

R. Castro-Beltrán, H. Desirena, G. Ramos-Ortiz, E. De la Rosa, G. Lanty et al.

Citation: *J. Appl. Phys.* **110**, 083110 (2011); doi: 10.1063/1.3654018

View online: <http://dx.doi.org/10.1063/1.3654018>

View Table of Contents: <http://jap.aip.org/resource/1/JAPIAU/v110/i8>

Published by the [American Institute of Physics](#).

Related Articles

In-plane thermal conductivity determination through thermorefectance analysis and measurements
J. Appl. Phys. **110**, 084313 (2011)

Tuning of a cavity in a silicon photonic crystal by thermal expansion of an elastomeric infill
Appl. Phys. Lett. **99**, 111113 (2011)

Assessing the thermal conductivity of non-uniform thin-films: Nanocrystalline Cu composites incorporating carbon nanotubes
J. Appl. Phys. **110**, 023506 (2011)

Strong absorption and selective thermal emission from a midinfrared metamaterial
Appl. Phys. Lett. **98**, 241105 (2011)

Nanothermochromics with VO₂-based core-shell structures: Calculated luminous and solar optical properties
J. Appl. Phys. **109**, 113515 (2011)

Additional information on *J. Appl. Phys.*

Journal Homepage: <http://jap.aip.org/>

Journal Information: http://jap.aip.org/about/about_the_journal

Top downloads: http://jap.aip.org/features/most_downloaded

Information for Authors: <http://jap.aip.org/authors>

ADVERTISEMENT

**AIP**Advances

Submit Now

**Explore AIP's new
open-access journal**

- **Article-level metrics
now available**
- **Join the conversation!
Rate & comment on articles**

Third-order nonlinear optical response and photoluminescence characterization of tellurite glasses with different alkali metal oxides as network modifiers

R. Castro-Beltrán,¹ H. Desirena,^{1,2} G. Ramos-Ortiz,^{1,a)} E. De la Rosa,^{1,a)} G. Lanty,³ J. S. Lauret,³ S. Romero-Servín,¹ and A. Schülzgen²

¹Centro de Investigaciones en Óptica León, A.P. 1-948, León, Gto. 37000, Mexico

²School of Optics and Center for Research and Education in Optics and Lasers, University of Central Florida, Orlando, Florida 32816-2700, USA

³Laboratoire de Physique de la Matière Condensée, Ecole Normale Supérieure, Paris Cedex 05, France

(Received 8 July 2011; accepted 15 September 2011; published online 24 October 2011)

Studies of the third-order nonlinear optical properties in $\text{TeO}_2\text{-MO-R}_2\text{O}$ glasses with three different alkali metal oxides $R_2\text{O}$ ($R = \text{Li, Na, K}$) as network modifiers and two network intermediates MO ($M = \text{Zn, Mg}$) are reported. The influence of such modifiers and intermediates on the nonlinear optical properties of these glasses was investigated using the standard Z-scan and the thermally managed Z-scan techniques under femtosecond pulse excitation at 800 nm. For different modifiers and intermediates, the nonlinear refraction indices n_2 of these glasses varied in the range 1.31–2.81 ($\times 10^{-15} \text{ cm}^2/\text{W}$). It was found that n_2 increases as the ionic radius of both network modifiers and intermediates decreases. Furthermore, the measurements show that the contribution from thermo-optical effects to the nonlinear refraction index is negligible for all of the studied glass compositions. In addition, the effect of modifiers and intermediates in the formation of localized states in the vicinity of the optical bandgap was also studied through photoluminescence experiments. These experiments revealed the presence of two emission bands (red and blue) originating from these localized states that can be populated after optical excitation and subsequent relaxation.

© 2011 American Institute of Physics. [doi:10.1063/1.3654018]

I. INTRODUCTION

Recently, TeO_2 -based optical glasses have received much attention for applications, such as laser devices, broadband amplifiers, up-conversion emission, and photonic crystal fibers.^{1–6} Furthermore, tellurite glasses exhibit large nonlinear (NL) refractive indices n_2 , which is a desirable property for all-optical switching devices.^{7–11} For this photonic application, tellurite glasses offer advantages over both semiconductors and organic materials because of their good transmission in the visible and infrared regions (up to 6 μm), fast response times, good mechanical properties, as well as affordability and processability. Moreover, when compared with other glass families, tellurites offer relatively low phonon energies and are mostly less toxic and more chemically and thermally stable.^{4–12}

In the development of tellurite glasses for optical signal processing and all-optical switching applications, it is necessary to combine large NL refractive indices with desirable thermo-mechanical properties. These optical and thermo-mechanical properties depend on the glass composition, and consequently, it results of interest to know how they are affected by the use of different glass formers and various possible network modifiers. Recently, a lot of work on composition and material properties has been reported for different glass families. For instance, the incorporation of alkali

metals as network modifiers has been studied in order to improve the thermo-mechanical properties as well as the optical properties.^{10–17} In regard to tellurite glasses, we recently reported the effect of alkali metal oxides $R_2\text{O}$ ($R = \text{Li, Na, K, Rb, and Cs}$) and network intermediates MO ($M = \text{Zn, Mg, Ba, and Pb}$) on the thermo-mechanical and chemical properties.¹⁸ In this study, the experimental results showed that alkali metals with small ionic radii decrease the thermal expansion coefficient, the glass transition temperature (T_g), and the chemical durability. As for the optical properties, the results showed that small ionic radii also favor the increase of the linear refractive index n , while third-harmonic generation (THG) experiments demonstrated also an increase in the nonlinear third-order susceptibilities of the type $\chi^{(3)}(-3\omega, \omega, \omega, \omega)$ for fundamental wavelength at 1550 nm. It is worth mentioning that THG is an easy technique for a quick screening of nonlinearities in optical materials, but it does not provide the value of the NL refractive index n_2 , the latter parameter being of paramount interest for all-optical switching applications. Motivated by this fact, in this work, we present direct measurements of n_2 for a series of TeO_2 glasses composed of various network modifiers and intermediates.

To explore the effect of alkali metals and network intermediates on the nonlinear refractive index of tellurite glasses, compositions, such as $\text{TeO}_2\text{-MO-R}_2\text{O}$, were studied. For this purpose, four TeO_2 -based glasses were prepared in a way that they all had the same molar concentration of TeO_2 . The magnitude of the NL refractive index n_2 was determined

^{a)}Authors to whom correspondence should be addressed. Electronic addresses: garamoso@cio.mx and elder@cio.mx.

using the standard Z-scan technique.¹⁹ Additionally, the thermally managed (TM) Z-scan technique²⁰ was also employed in order to identify possible contributions to n_2 from thermo-optical effects. Note that the use of different network modifiers and intermediates in tellurite glasses introduces changes in the coefficient of thermal expansion which can influence the overall nonlinear response. Therefore, we applied a TM Z-scan technique that enables one to discriminate between nonlinearities of pure electronic origin and nonlinearities due to accumulative thermal effects. This information is important, since only nonlinear electronic processes can provide fast material response (fs to ps), which is of interest for photonic application, including optical processing of information.

Finally, to obtain more information about the electronic structure in tellurite glasses, the effect of modifiers and intermediates on the formation of localized states was also studied through photoluminescence and pump-probe experiments.

II. EXPERIMENTS

A. Nonlinear materials

The glasses studied here with composition (mol. %) $70\text{TeO}_2\text{-}20\text{MO-}10\text{R}_2\text{O}$ were prepared using the conventional method of powder melting and annealing process as reported elsewhere.¹⁸ The network intermediates are $M = \text{zinc (Zn)}$ or magnesium (Mg) , and the network modifiers are $R = \text{lithium (Li)}$, sodium (Na) , and potassium (K) . Reagent-grade tellurium oxide (TeO_2), zinc oxide (ZnO), magnesium oxide (MgO), potassium carbonate (K_2CO_3), sodium carbonate (NaCO_3), and lithium oxide (Li_2O) were used as starting materials. Calculated quantities of chemicals were mixed in a glass dish and melted in an electric furnace at 900°C for one hour using an alumina crucible. Each melt was cast into a preheated aluminum mold with a size of $5 \times 13 \times 13 \text{ mm}^3$. Subsequently, it was removed from the mold and transferred to a furnace for annealing process at a temperature from 270°C to 380°C , depending on the glass composition, for approximately 21 h. For characterization, the samples were cut and polished to obtain $\sim 1 \text{ mm}$ thick slabs. Special care was taken to polish the samples in order to reduce errors in Z-scan experiments due to glass imperfections. The glass compositions and code used in this work for each sample are summarized in Table I. This table also shows the linear refractive index at 800 nm obtained from calculated dispersion curves that resulted from direct measurements of the refractive index at 633, 830, and 1550 nm through the use of the prism coupler technique.¹⁸

TABLE I. Code, glass composition (mol. %), and refractive index for the tellurite glasses used in this study.

Glass	TeO ₂	ZnO	MgO	K ₂ O	Na ₂ O	Li ₂ O	n (800 nm)
TeZnK	70	20	—	10	—	—	1.887
TeZnNa	70	20	—	—	10	—	1.918
TeZnLi	70	20	—	—	—	10	1.956
TeMgLi	70	—	20	—	—	10	1.919

B. Z-scan

The Z-scan technique was used to characterize the NL optical properties of the tellurite glasses. This technique is based on the NL phase measurement of a laser beam propagating through the sample under study and provides a sensitive method to measure the real and imaginary parts of the complex NL refractive index.¹⁹ Different physical mechanisms, i.e., thermal and nonthermal, can contribute significantly to the measured values of n_2 . For photonic glasses, only electronic (nonthermal) nonlinearities are required; therefore, it is necessary to anticipate the contributions of induced thermal lensing effects on the value of n_2 . In order to discriminate between the thermal and electronic nonlinearities, Gnoli *et al.*²⁰ introduced a modification to the standard Z-scan technique, the so-called TM Z-scan. In brief, it involves the time evolution measurement of the normalized transmittance at the valley and the peak of a Z-scan signal that is obtained using a femtosecond laser with a high repetition rate. To do this, a laser beam is modulated by a mechanical chopper placed in the focus of a Keplerian telescope. Using this modulated beam in the Z-scan set-up results in a temporal resolution of the system that is determined by the chopper opening time. In our case, special care has been taken to produce a resolution of $10 \mu\text{s}$ by a right combination of the finite size of the beam waist in the Keplerian telescope, special modification in the slots of the chopper wheel, and the angular velocity of the chopper wheel. The so-obtained resolution time was about double with respect to the values reported by other authors.^{11,20–22} By extrapolating the time-resolved Z-scan signals to the time $t = 0$ (determined by the opening time of the chopper), the change in normalized transmittance between peak and valley has been obtained at very early times before thermal effects start to influence the Z-scan signal. From these extrapolated values, the nonthermal NL refractive indices have been calculated. In the present work, the TM Z-scan was implemented using pulses of 100 fs duration centered at 800 nm. The pulse trains with 80 MHz repetition rate have been generated by a Ti:sapphire oscillator (Tsunami, Spectra-Physics). With this oscillator, typical peak intensities at the sample position were in the range of $1\text{--}10 \text{ GW/cm}^2$. In these experiments, the Rayleigh length was 2.45 mm and the aperture transmittance at far field was $S = 0.4$. The glass characterization was also performed with the standard Z-scan technique, applying higher intensity pulses with 280 fs duration from a femtosecond Ti:sapphire regenerative amplifier at 1 KHz repetition rate.

C. Photoluminescence and pump-probe experiments

Photoluminescence (PL) spectra from tellurite glass samples were obtained after excitation with the third-harmonic (355 nm) of a pulsed Nd:YAG laser (7 ns pulses at 10 Hz repetition rate) and with the second-harmonic (244 nm) of a continuous wave argon laser. In addition, the dynamics of electronic excitations in the glasses were studied through time-resolved pump-probe experiments. In this case, the transient change of transmission of the samples was measured in a non-degenerate setup employing femtosecond pump pulses at 440 nm (2.8 eV) with typical intensities in the range of

0.38–1.2 mJ/cm² and probe pulses at 516 nm (2.4 eV) with intensities a hundred times weaker with respect to pump pulses. The instrument response was evaluated through the cross correlation between the pump and probe pulses and gave a temporal resolution of 120 fs.

III. RESULTS AND DISCUSSIONS

A. Absorption and optical bandgap

To estimate the optical bandgap of the samples, linear absorption measurements have been performed. The absorption spectra were measured from 300 to 3000 nm using a spectrophotometer (Lambda 900, Perkin-Elmer) and are shown in Fig. 1. The tellurite glasses were optically transparent in the range of wavelengths from 450 nm (2.75 eV) to 2500 nm (0.49 eV), while a weak tail of linear absorption was present at 400 nm (3.10 eV). The optical bandgap energy E_g for each sample was obtained from its absorption spectrum, following the Tauc approach.²³ By plotting $\sqrt{\alpha \cdot h\nu}$ as a function of photon energy $h\nu$ (α is the absorption coefficient in cm⁻¹) and extrapolating the linear regions of this function to zero absorption, optical bandgap values of 3.55 eV, 3.59 eV, 3.50 eV, and 3.48 eV were obtained for TeZnK, TeZnNa, TeZnLi, and TeMgLi, respectively. These values are larger than those reported in the literature for pure TeO₂ glasses, which are in the range 3.15–3.37 eV,^{24,25} which means that the inclusion of modifiers and network intermediates shifts the bandgap to higher energies. Our samples also show larger E_g than in tellurite glasses that use Bi as a network intermediate, i.e., TeO₂-Bi₂O₃-ZnO,²⁶ but are smaller than those reported for rare earth-doped tellurite glasses.²⁴

B. Nonlinear optical properties

The samples exhibited a self-focusing effect in the Z-scan experiments. In Fig. 2(a), examples of Z-scan traces for TeZnNa and TeZnK glasses are shown. Here, a peak preceded by a valley in the normalized transmittance clearly indicates

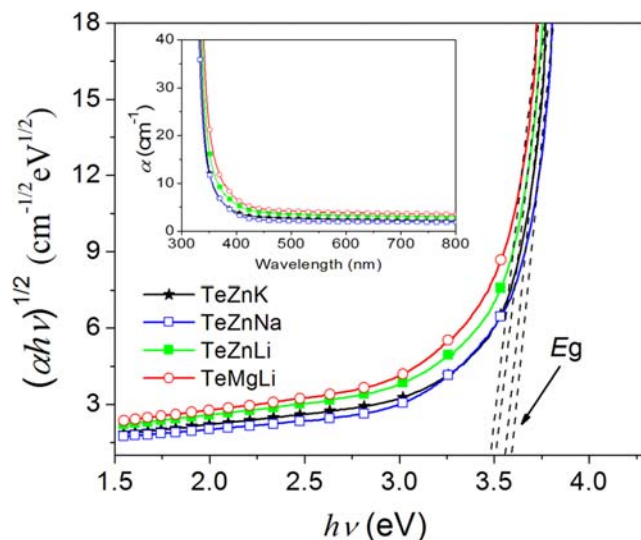


FIG. 1. (Color online) Dependence of $(\alpha \cdot h\nu)^{1/2}$ on the photon energy for tellurite glasses. Inset: absorption spectra of the tellurite glasses.

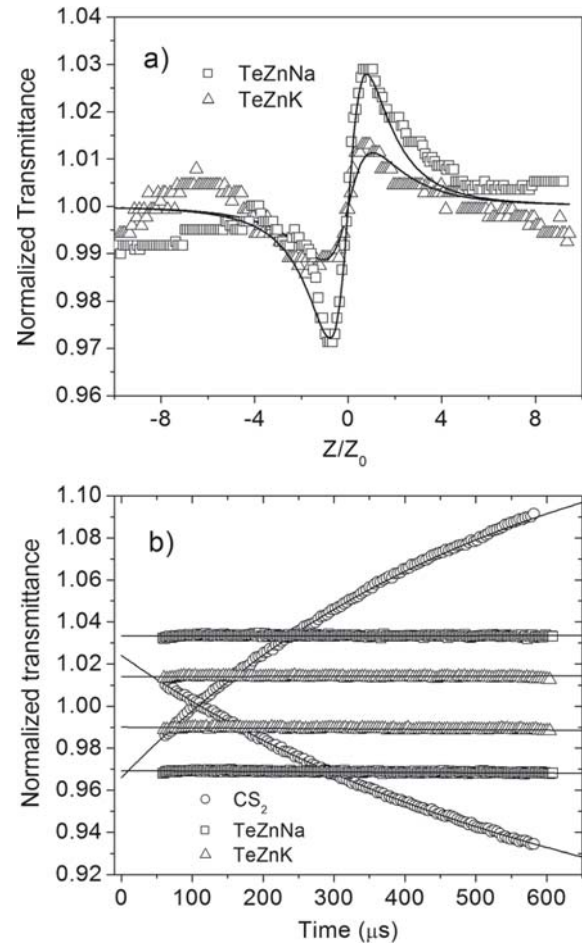


FIG. 2. (a) Normalized transmittance of standard Z-scan measurements for TeZnNa and TeZnK. The continuous lines are fittings to the experimental data. (b) Thermally managed Z-scan signals at valleys and peaks of traces shown in (a). The traces of CS₂ are included as reference.

that glasses have a positive NL refractive index. These traces were obtained with a train of fs pulses at high repetition rate from the Ti:sapphire oscillator with a peak intensity of 9.0 GW/cm² at the sample position. Figure 2(b) shows the temporal evolution of the TM Z-scan signals at the positions of minimum (valley) and maximum (peak) transmittance for these two glasses. The signals exhibit negligible time evolution. The changes in normalized transmittance between peak and valley immediately after excitation have been obtained by extrapolating the evolution curves to the time $t=0$, and the corresponding electronic values of n_2 have been found to be 1.31 and 2.33 ($\times 10^{-15}$ cm²/W) for TeZnK and TeZnNa, respectively. Figure 2(b) also shows the signal obtained from the standard reference CS₂ (contained in a ~ 1 mm quartz cell). In this case, the crossing of the two TM Z-scan curves reveals the presence of both self-focusing (electronic) and self-defocusing (thermal) effects that compete during the time that the sample is exposed to the train of fs pulses. It is evident that, in CS₂, the electronic nonlinear response dominates at early times, but the thermal nonlinearity dominates over the electronic response of the material after ~ 100 μ s, as shown by the crossing of the TM Z-scan curves at such time. By extrapolating the evolution curves of CS₂, the electronic value of n_2 resulted to be 2.11×10^{-15} cm²/W, which is in good agreement

TABLE II. Values of n_2 and the third-order nonlinear susceptibility $\chi^{(3)}(-\omega; \omega, -\omega, \omega)$ measured through thermally managed Z-scan technique.

Sample	$n_2 [10^{-15} \text{cm}^2/\text{W}]$	$\chi^{(3)} (10^{-13} \text{esu})$
TeZnK	1.31 ± 0.20	1.15
TeZnNa	2.33 ± 0.42	2.06
TeZnLi	2.37 ± 0.40	2.10
TeMgLi	2.81 ± 0.5	2.5
CS ₂	2.11 ± 0.45	1.87

with values previously reported for this material²⁷ and, thus, validates the calibration of our experimental apparatus. Following this procedure, the n_2 values for glasses TeZnLi and TeMgLi were found to be 2.37 and 2.81 ($\times 10^{-15} \text{ cm}^2/\text{W}$), respectively. For these glasses also, no temporal evolution of the TM Z-scan signal was observed. Table II summarizes the NL refractive indices determined for our tellurite glasses as well as the real part of the third-order nonlinear susceptibility $\chi^{(3)}(-\omega, \omega, \omega, \omega)$. Both quantities are related through $n_2 = 3\chi^{(3)}/4\epsilon_0 n^2 c$, where n is the linear refractive index.

The absence of a temporal evolution in the TM Z-scan signals from the tellurite glasses studied in this work clearly shows that their third-order optical nonlinearity originated from pure electronic polarization. By examining Table II for the glasses with the network intermediate Zn, it is observed that n_2 increases in the following order $\text{TeZnK} < \text{TeZnNa} < \text{TeZnLi}$, although the sample with Li as modifiers is barely larger than in the case of Na. A further increase of nonlinearity is also observed when Zn is replaced by Mg as intermediate. The nonlinear response is related with the degree of hyperpolarizability of the sample as a result of the structural changes inside the arrangement with the presence of modifiers and intermediates. Therefore, the trend exhibited by samples with Zn as intermediate can be attributed to the decrease in ionic radius from K to Li through Na that leads to a modification of the polarizability per unit volume.²⁸ Similarly, the nonlinear response increases when Zn is substituted by Mg, which has a smaller ionic radius. From this concept, it follows that the number of ions per unit volume might increase as the ionic radii of the network modifiers and/or intermediates decrease. The corresponding ion radii for K, Na, Li, Zn, and Mg are 1.33, 0.95, 0.68, 0.74, and 0.65 Å, respectively. Thus, more ions per unit volume can be polarized using Li and Mg as modifier and intermediate, respectively, and consequently, the nonlinear response is larger. In the opposite case, fewer ions per unit volume can be polarized with the use of K and Zn, and consequently, the nonlinear response is weaker (see Table II). This trend was also observed in the nonlinear susceptibilities of the type $\chi^{(3)}(-3\omega, \omega, \omega, \omega)$ measured by means of THG at 1.9 μm for binary glasses of the type $\text{TeO}_2\text{-R}_2\text{O}$ with $R = \text{K, Na, Li}$.²⁸ As for ternary glasses, a recent study on the optical properties of codoped tellurite glasses based in the matrix $\text{TeO}_2\text{-ZnO-Na}_2\text{O}$ showed a NL refractive index of $1.90 \times 10^{-15} \text{ cm}^2/\text{W}$ at 800 nm.¹¹ The matrix reported in that work was similar to our TeZnNa sample, although with a concentration of 5 mol. % for the modifier Na₂O (and 20 mol. % for ZnO). Thus, the values of n_2 measured in the present work for TeZnNa and in Ref. 11 for a similar glass composition show good agreement.

The NL refractive index for the series of glasses with Zn as the network intermediate followed the order suggested by the semiempirical Miller's rule (stating that materials with larger linear refractive index possess larger NL refractive index), although they do not vary in proportion to the variation of their linear refractive index. However, the rule fails with the introduction of Mg as the network intermediate (see Table II). According to Miller's rule, TeMgLi shows an unexpected larger nonlinearity in comparison to TeZnLi, being their linear refractive index 1.919 and 1.956 at 800 nm, respectively. In this case, the nonlinearity increased when Zn was replaced by Mg in the glass composition to obtain a maximum value of $2.81 \times 10^{-15} \text{ cm}^2/\text{W}$. This is not surprising, as other authors have also observed the failure of Miller's rule.^{29,30} Further, in our previous work,¹⁸ it was also observed that the introduction of Mg to replace Zn in the glass composition increased the third-order susceptibility tensor associated with the optical nonlinear effect of third-harmonic generation for infrared wavelengths.

The Z-scan experiments demonstrate that the glass composition of our samples not only exhibit large values of n_2 , but also have a good capacity to disperse the absorbed heat, precluding the appearance of accumulative thermal effects (thermal lensing) that could affect the nonlinear optical behavior. In our case, heat is produced from the residual linear absorption at 800 nm (at this wavelength, NL absorption was not experimentally detected for the maximum peak powers available in our TM Z-scan experiment). The absorption coefficient was estimated to be in the range of 0.1–1 cm^{-1} , depending on the sample, and was calculated from the linear absorption spectra once the reflection losses were taken into account (typical transmittance in these glasses is about 80%). The capacity of the samples to disperse the absorbed heat was tested in various experimental conditions. For instance, it is worth to mention that, in the TM Z-scan experiments, the illumination time was ~ 1 ms (the time allowed for the chopper wheel to excite the sample) followed by ~ 36 ms without illumination. This duty cycle was varied by simply changing the frequency of the chopper wheel, and no appreciable thermal effect was detected, even for longer times of illumination. Furthermore, standard Z-scan experiments were performed using a continuous wave titanium:sapphire laser with 400 mW output power. In this case, a constant transmittance was observed and no evidence of thermal lensing was detected. These results are interesting in view of the thermo-optical response measured in other glasses with different techniques. For instance, in binary and ternary tellurite glasses with composition (in mol. %) 80TeO₂–20Li₂O and 80TeO₂–15Li₂O–5TiO₂ and with similar residual absorption than those corresponding to our samples ($\sim 1 \text{ cm}^{-1}$), a small thermal lens effect was detected under cw Ar⁺ laser excitation with 81 mW at 514 nm.³¹

The values of NL refractive index n_2 for the tellurite glasses were independent of the peak intensities available for the laser oscillator used in the TM Z-scan experiments. In order to study the nonlinear response at much higher intensities, we analyzed the samples using the standard Z-scan under fs pulses delivered by a Ti:sapphire regenerative amplifier. Figure 3 shows an example of the nonlinear response of

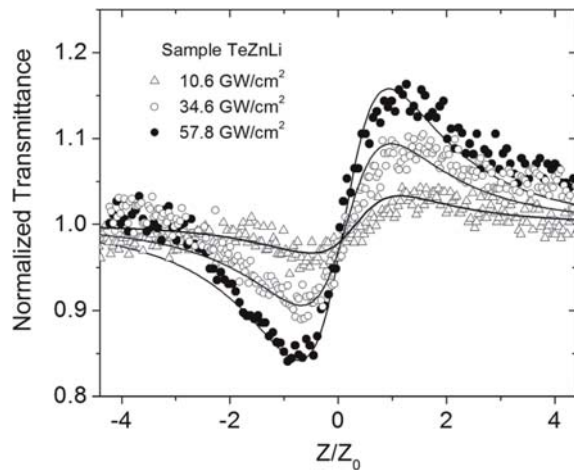


FIG. 3. Normalized transmittance in standard Z-scan measurements for TeZnLi under femtosecond excitation at 1 KHz pulse repetition rate and different intensities. The continuous lines are fittings to the experimental data.

the TeZnLi sample at three different peak intensities: 10.6, 34.6, and 57.8 GW/cm^2 . From these Z-scan traces, the values of n_2 resulted in 2.51, 2.24, and 2.07 ($\times 10^{-15} \text{ cm}^2/\text{W}$), respectively, showing that at high peak intensities, the nonlinear response saturates. Figure 4 presents the values of the NL refractive index measured for all samples under study at 10.6 and 57.9 GW/cm^2 , and for comparison, the figure includes those values obtained with TM Z-scan at 9.0 GW/cm^2 . Notice the good agreement between the values of n_2 obtained at 10.6 GW/cm^2 with a train of pulses at 1 KHz and those obtained through TM Z-scan at 9.0 GW/cm^2 with a train of pulses at 80 MHz. This confirms that the nonlinear response is free of accumulative thermal lensing effects, even upon excitation at high frequencies of repetition rate with intensities of the order of 10 GW/cm^2 . Moreover, at this level of intensities, the experiment with pulses at 1 KHz also demonstrates (see Fig. 4) that the order in which the nonlinearities increase as a function of the modifiers is the same as that observed in TM Z-scan experiments. However, when the peak intensities are

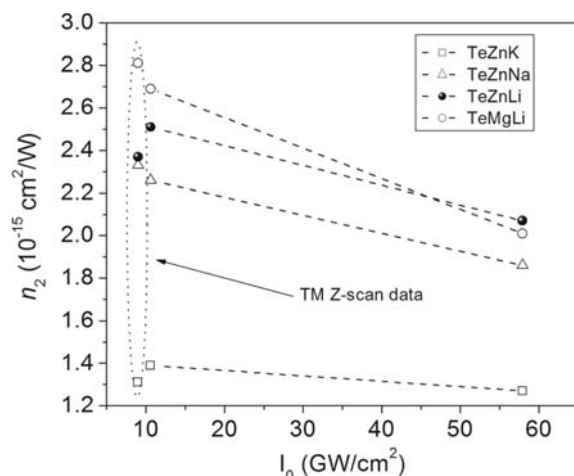


FIG. 4. Variation of n_2 as a function of intensities obtained under femtosecond excitation at 1 KHz pulse repetition rate. For comparison, the values of n_2 obtained through TM Z-scan experiments at 80 MHz pulse repetition rate are included.

further increased, the values of n_2 decrease to some extent, as it is observed in Fig. 4 for the intensity of 57.8 GW/cm^2 . The decrease of the measured NL refractive indices at very high intensities might be associated with the appearance of nonlinearities of higher order or another physical process that modifies the material response. Nevertheless, it is worth to point out that, during these experiments, the glasses did not reveal apparent optical damage. This suggests that our samples are able to withstand high optical peak intensities without showing optical damage.

C. Photoluminescence and transient absorption

In Fig. 5, the PL of TeZnLi after UV excitation is shown. Clearly, position and structure of the emission bands change, depending on the excitation wavelength. All tellurite glass samples exhibited very similar emission spectra independently of the modifier or network intermediate in their composition, although TeZnLi showed the most intense PL signal. Low pump intensities were used to obtain these spectra. Figure 5 shows a red emission band centered at 650 nm (1.90 eV) with a bandwidth of 140 nm after excitation at 355 nm (3.49 eV) and a blue emission band centered at 437 nm (2.83 eV) and with a bandwidth of 83 nm after excitation at 244 nm (5.08 eV). Both emission bands are the result of electron relaxation from electronic states, with energies lying within the bandgap, as illustrated in the energy scheme in Fig. 6, where ETb and ETc stand for the states responsible for blue and red emission bands, respectively. Those localized electronic states were produced by defects induced during the glass fabrication and can be probably related to the presence of both modifiers and network intermediates. Blue emission is likely associated with the presence of oxygen vacancies ($\Delta E_g \sim 2.8 \text{ eV}$), as has been described for ZnO ,³² while the red emission is probably associated with sites where the modifiers (Li, Na, K) constitute impurities.^{33,34} The observed PL dependence on the wavelength of excitation suggests two mechanisms for electronic transitions. Excitation at 355 nm promotes electrons from the valence band to the conductive band edge, and after nonradiative relaxations, ETc is populated; subsequently,

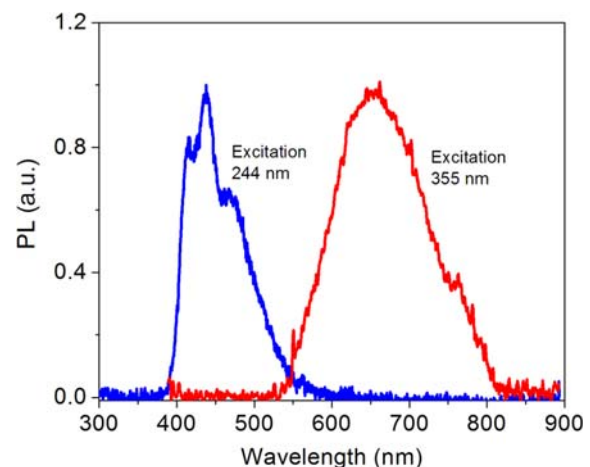


FIG. 5. (Color online) Normalized photoluminescence spectra for sample TeZnLi after excitation with 244 nm and 355 nm laser light.

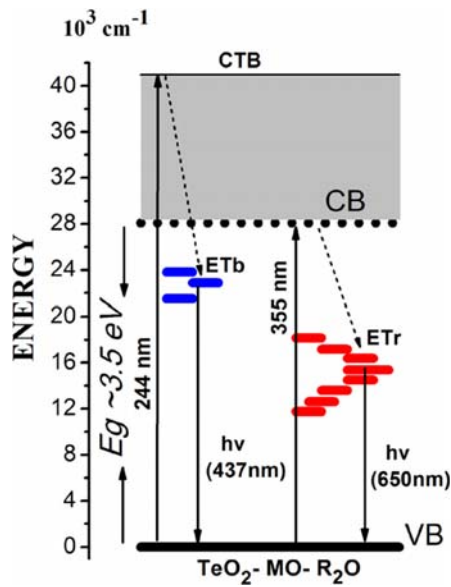


FIG. 6. (Color online) Schematic energy level diagrams for tellurite glasses. Dotted lines indicate nonradiative relaxations.

radiative decays generate the red PL band. For 244-nm excitation, the charge transfer band (CTB) is populated and successive nonradiative relaxations result in the population of the ETb state, which generates the blue PL band. This is in agreement with the analysis of the CTB in TeO_2 glasses reported previously.^{35,36}

To study the dynamics of the excited states, we performed nondegenerate pump-probe experiments with wavelengths corresponding to photon energies smaller than the optical bandgap. The samples were excited by strong pump pulses at 440 nm (2.8 eV), while delayed and weak probe pulses at 516 nm (2.4 eV) allowed us to measure transient changes of transmission ΔT induced by the pump pulses. The change in transmission is defined as $\Delta T = T_p - T$, where T_p and T are the transmission with and without pump, respectively. Figure 7 displays $\Delta T/T$ as a function of time delays between pump and probe pulses for the samples TeZnK, TeZnNa, TeZnLi, and TeMgLi. In this figure, the major component is a fast transient-induced absorption (i.e., decrease of transmission or negative values of $\Delta T/T$) of few hundreds of fs and a long and weak tail. This suggests that the decrease of $\Delta T/T$ observed in all the samples might be associated with induced absorption from the localized states to the conduction band. Notice that the wavelength of the pump corresponds to an energy (2.8 eV) that is below the optical bandgap (3.5 eV) of samples and thus excitation can only occur into the localized states, and from them, subsequent absorption of the probe beam promotes electrons to the conduction band. According to the excitation energies used in these experiments, the detected transient absorption should be mostly related to the localized states ETb. The transient absorption and dynamics of the localized states ETr were not obtained, since our excitation system could not be tuned to proper wavelength (~ 1.90 eV). Figure 7 also shows the presence of a fast $\Delta T/T$ increase ($\Delta T/T > 0$) just for early delays. In this case, that component of transient transmission

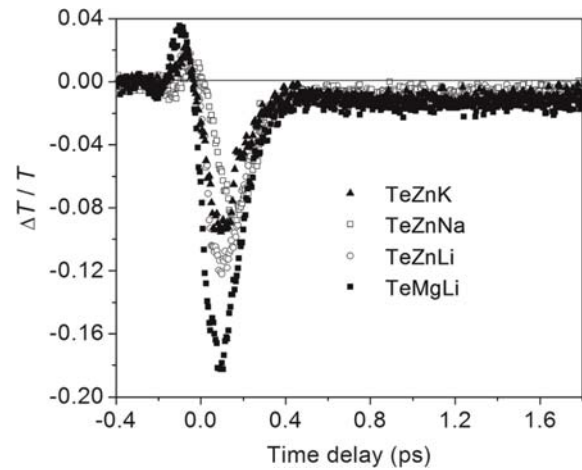


FIG. 7. Transient changes of transmission of samples for pump pulses at 440 nm (2.8 eV) and probe pulses at 516 nm (2.4 eV).

might not represent population dynamics of electronic states, but a coherent artifact produced by third-order nonlinear effects, i.e., cross phase modulation effects. In any case, these experiments confirm the existence of localized states and also demonstrate the fast response of the material.

Finally, it is expected that the localized states have a small effect on the nonlinearities of the glasses at nonresonant frequencies, i.e., those optical frequencies at which Z-scan experiments were performed. Note that the optical bandgap in glasses plays a role in defining the magnitude of their nonlinearities, for example, it has been observed that nonlinearities increase as the energy gap decreases.^{25,28} Thus, according to this description, the localized states of our tellurite glasses, as well as other disorders in amorphous materials, only produce weak absorption tails in the forbidden energy band, so that they should not modify substantially the nonlinear response. Nevertheless, for optical frequencies in resonance, the localized states can induce enhanced nonlinearities, i.e., multiphoton absorption.

IV. CONCLUSIONS

The third-order NL optical behavior of tellurite-based glasses with three different alkali metal oxides R_2O ($R = \text{Li}, \text{Na}, \text{K}$) as network modifiers and ZnO and MgO as network intermediates was investigated. It was found that the third-order nonlinear optical response at 800 nm is due to the electronic polarization with negligible thermo-optical contribution. The maximum NL refractive index of $n_2 = 2.81 \times 10^{-15} \text{ cm}^2/\text{W}$ was obtained for samples with Li as modifier and Mg as intermediate. This large n_2 value is attributed to an increase in hyperpolarizability of samples with Li and Mg as a result of their small ionic radii. All glasses exhibit two visible emission bands which can be excited through different excitation wavelengths. Both emission bands originate from optical transitions that include electronic states with smaller energies than the optical bandgap of the tellurite glasses. Those bands are associated to defects produced during the glass fabrication and the presence of modifiers. The presence of such defect states was confirmed by pump-probe experiments. Our experimental results provide new

information to gain understanding on the nonlinear and luminescent properties of tellurite glasses. It is demonstrated that TeO₂-MO-R₂O glasses, whose properties can be optimized by changing the modifiers, are excellent candidates for all-optical switching devices operating in the near infrared.

ACKNOWLEDGMENTS

This work was partially supported by CONACyT (Ref. J49512-F) and CONCYTEG (Ref. 09-04-K662-072 and 09-04-K662-055). R.C.-B., H.D. and S.R.-S. acknowledge CONACyT for Ph.D. scholarships.

- ¹R. Rolli, M. Montagna, S. Chausseidant, A. Monteil, V. K. Tikhomirov, and M. Ferrari, *Opt. Mater.* **21**, 743 (2003).
- ²J. Jackson, C. Smith, J. Massera, C. Rivero-Baleine, C. Bungay, L. Petit, and K. Richardson, *Opt. Express* **17**, 9071 (2009).
- ³S. Shen, A. Jha, X. Liu, M. Naftaly, K. Bindra, H. J. Bookey, and A. K. Kar, *J. Am. Ceram. Soc.* **85**, 1391 (2002).
- ⁴X. Feng, W. H. Loh, J. C. Flanagan, A. Camerlingo, S. Dasgupta, P. Petropoulos, P. Horak, K. E. Frampton, N. M. White, J. H. Price, H. N. Rutt, and D. J. Richardson, *Opt. Express* **16**, 13651 (2008).
- ⁵P. V. dos Santos, M. V. D. Vermelho, E. A. Gouveia, M. T. de Araújo, F. C. Cassanjes, S. J. L. Ribeiro, and Y. Messaddep, *J. Chem. Phys.* **116**, 6772 (2002).
- ⁶S. Xu, H. Ma, D. Fang, Z. Zhang, and Z. Jiang, *Mater. Lett.* **59**, 3066 (2005).
- ⁷M. Dutreilh-Colas, P. Thomas, and J. C. Champarnaud-Mesjard, *Phys. Chem. Glasses* **44**, 349 (2003).
- ⁸F. Chen, T. Xu, S. Dai, Q. Nie, X. Shen, J. Zhang, and X. Wang, *Opt. Mater.* **32**, 868 (2010).
- ⁹A. P. Mirgorodsky, M. Soulis, P. Thomas, and T. Merle-Méjean, *Phys. Rev. B* **73**, 134206 (2006).
- ¹⁰R. F. Souza, M. A. R. C. Alencar, J. M. Hickmann, R. Kobayashi, and L. R. P. Kassab, *Appl. Phys. Lett.* **89**, 171917 (2006).
- ¹¹F. Eroni, P. dos Santos, F. C. Fávero, A. S. L. Gomes, J. Xing, Q. Chen, M. Fokine, and I. C. S. Carvalho, *J. Appl. Phys.* **105**, 024512 (2009).
- ¹²J. C. McLaughlin, S. L. Tagg, and J. W. Zwanziger, *J. Phys. Chem. B* **105**, 67 (2001).
- ¹³J. S. Wang, E. M. Vogel, and E. Snitzer, *Opt. Mater.* **3**, 187 (1994).
- ¹⁴H. Lin, S. Jiang, J. Wu, F. Song, N. Peyghambarian, and E. Y. B. Pun, *J. Phys. D: Appl. Phys.* **36**, 812 (2003).
- ¹⁵Y. Gao and C. Cramer, *Solid State Ionics* **176**, 2279 (2005).
- ¹⁶S. P. Singh, Aman, and A. Tarafder, *Bull. Mater. Sci.* **27**, 281 (2004).
- ¹⁷H. Takebe, Y. Nageno, and K. Morinaga, *J. Am. Ceram. Soc.* **77**, 2132 (1994).
- ¹⁸H. Desirena, A. Schülzgen, S. Sabet, G. Ramos-Ortiz, E. de la Rosa, and N. Peyghambarian, *Opt. Mater.* **31**, 784 (2009).
- ¹⁹M. Sheik-Bahae, A. A. Said, and E. W. Van Stryland, *Opt. Lett.* **14**, 955 (1989).
- ²⁰A. Gnoli, L. Razzari, and M. Righini, *Opt. Express* **13**, 7976 (2005).
- ²¹F. E. P. dos Santos, C. B. de Araújo, A. S. L. Gomes, K. Fedus, G. Boudebs, D. Manzani, and Y. Messaddep, *J. Appl. Phys.* **106**, 063507 (2009).
- ²²A. S. L. Gomes, E. L. Falcão Filho, and C. B. de Araújo, *Opt. Express* **15**, 1712 (2007).
- ²³J. Tauc, R. Grigorovici, and A. Vancu, *Phys. Status Solidi* **15**, 627 (1966).
- ²⁴L. M. Sharaf El-Deen, M. S. Al Sallhi, and M. M. Elkholy, *J. Alloys Compd.* **465**, 333 (2008).
- ²⁵S.-H. Kim, T. Yoko, and S. Sakka, *J. Am. Ceram. Soc.* **76**, 2486 (1993).
- ²⁶E. Yousef, M. Hotzel, and C. Rüssel, *J. Non-Cryst. Solids* **353**, 333 (2007).
- ²⁷R. A. Ganeev, A. I. Rysanyansky, M. Baba, M. Suzuki, N. Ishizawa, M. Turu, S. Sakakibara, and H. Kuroda, *Appl. Phys. B* **78**, 433 (2004).
- ²⁸S.-H. Kim, *J. Mater. Res.* **14**, 1074 (1999).
- ²⁹Q. Liu, C. Gao, H. Zhou, B. Lu, X. He, Q. Shixiong, and X. Zhao, *Opt. Mater.* **32**, 26 (2009).
- ³⁰H. Guo, H. Tao, S. Gu, X. Zheng, Y. Zhai, S. Chu, X. Zhao, S. Wang, and Q. Gong, *J. Solid State Chem.* **180**, 240 (2007).
- ³¹S. M. Lima, W. F. Falco, E. S. Bannwart, L. H. C. Andrade, R. C. de Oliveira, J. C. S. Moraes, K. Yukimitu, E. B. Araújo, E. A. Falcão, A. Steimacher, N. G. C. Astrath, A. C. Bento, A. N. Medina, and M. L. Baesso, *J. Non-Cryst. Solids* **352**, 3603 (2006).
- ³²D. H. Zhang, Z. Y. Xue, and Q. P. Wang, *J. Phys. D: Appl. Phys.* **35**, 2837 (2002).
- ³³J. W. P. Hsu, D. R. Tallant, R. L. Simpson, N. A. Missert, and R. G. Cope-land, *Appl. Phys. Lett.* **88**, 252103 (2006).
- ³⁴S. A. Studenikin, N. Golego, and M. Cocivera, *J. Appl. Phys.* **84**, 2287 (1998).
- ³⁵R. P. Sreekanth Chakradhar, G. Sivaramaiah, J. Lakshmana Rao, and N. O. Gopal, *Mod. Phys. Lett. B* **19**, 643 (2005).
- ³⁶A. Berthereau, Y. Le Luyer, R. Olazcuaga, G. Le Flem, M. Couzi, L. Canioni, P. Segonds, L. Sarger, and A. Ducasse, *Mater. Res. Bull.* **29**, 933 (1994).